DRAFT VERSION AUGUST 10, 2001
Preprint typeset using LaTeX style emulateapj v. 14/09/00

UNDERSTANDING CLUSTER GAS EVOLUTION AND FINE-SCALE CMB ANISOTROPY WITH DEEP SUNYAEV-ZEL'DOVICH EFFECT SURVEYS

GILBERT P. HOLDER AND JOHN E. CARLSTROM
Department of Astronomy and Astrophysics, University of Chicago, Chicago, IL 60637
holder@oddjob.uchicago.edu,jc@hyde.uchicago.edu
Draft version August 10, 2001

ABSTRACT

We investigate the impact of gas evolution on the expected yields from deep Sunyaev-Zel'dovich (SZ) effect surveys as well as on the expected SZ effect contribution to fine scale anisotropy in the Cosmic Microwave Background. The approximate yields from SZ effect surveys are remarkably insensitive to gas evolution, even though the observable properties of the resulting clusters can be markedly different. The CMB angular power spectrum at high multipoles ($\ell \gtrsim 2000$, $\lesssim 5'$) due to the SZ effect from clusters is quite sensitive to gas evolution. We show that moderate resolution ($\leq 1'$) SZ effect imaging of clusters found in deep SZ effect surveys should allow a good understanding of gas evolution in galaxy clusters, independent of the details of the nature of the gas evolution. Such an understanding will be necessary before precise cosmological constraints can be set from yields of large cluster surveys.

Subject headings: cosmic microwave background — cosmology: theory — large-scale structure of universe — cosmological parameters

1. INTRODUCTION

The Sunyaev-Zel'dovich (SZ) effect has recently become a valuable observational tool (Birkinshaw 1999). In the past few years, observational programs have shifted from attempting to detect the effect to using the SZ effect to map out massive clusters of galaxies, study the intra-cluster medium (ICM), and constrain cosmological parameters (Carlstrom *et al.* 2000).

The thermal SZ effect is a distortion of the cosmic microwave background (CMB) spectrum caused by hot gas along the line of sight to the surface of last scattering. The cool CMB photons undergo Compton scattering on the hot electrons, gaining on average a small amount of energy in the process, creating an intensity decrement at low frequencies ($\nu \lesssim 218$GHz) and an increment at high frequencies.

Current instruments are now regularly detecting and imaging clusters at high signal-to-noise, and the next generation of instruments should be capable of mapping fairly large portions of the sky as a means of finding clusters of galaxies. Several works (e.g., Bartlett 2000; Holder *et al.* 2000; Barbosa *et al.* 1996; Kneissl *et al.* 2001) have predicted the number of clusters that could be expected in future SZ surveys and their angular power spectrum. The survey yields are quite impressive; the next generation of SZ instruments should be able to detect several clusters per day.

In this work, we take a slightly different perspective. Rather than asking how many clusters an SZ survey will find, we instead focus on which clusters we would like to find and what we can learn from these objects. We use simple models for the gas distribution of galaxy clusters to investigate the impact of non-gravitational heating on observable cluster properties, focusing on the SZ effect. Much work has gone into using the X-ray emission from nearby groups and low-mass clusters to constrain feedback from galaxy formation and non-gravitational heating (e.g., Bower *et al.* 2000; Cavaliere, Menci, and Tozzi 1999; Balogh, Babul, and Patton 1999) or alternatively the preferred cooling of low-entropy gas (Bryan 2000). The effects of feedback or cooling should be even more important at higher redshift and for low masses, where the SZ effect will be an important probe.

In §2 we outline our models and the important SZ observables. We show the expected SZ properties of clusters in §3 and angular power spectra for these models in §4. Finally, in §5, we discuss our results and implications for planned SZ surveys.

2. SZ EFFECT FROM GALAXY CLUSTERS

X-ray observations indicate that the cluster gas is approximately isothermal (Irwin and Bregman 2000), and that the gas density profile can be approximated by a "beta model" (Mohr, Mathiesen, and Evrard 1999):

$$\rho_g(r) = \frac{\rho_{g,\circ}}{[1+(r/r_c)^2]^{3\beta/2}} \quad , \tag{1}$$

where $\rho_{g,\circ}$ is the central gas density and r_c is a core radius. We choose to fix $\beta = 2/3$, with the knowledge that this will give a reasonable SZ profile even if the true SZ best-fit value of β for clusters is slightly higher (Reese *et al.* 2000; Grego *et al.* 2001). With this choice of β, the mass is divergent, and must be truncated at some radius. We set the truncation radius to be the virial radius, derived from the spherical collapse model, as outlined below.

For this cluster model, the central decrement of the cluster can be written as

$$\frac{\Delta T_\circ}{T_{CMB}} = f(\nu)\ y = 2f(\nu)\frac{kT_e}{m_e c^2}\sigma_T n_\circ r_c \arctan\left(\frac{R_v}{r_c}\right) \quad , \tag{2}$$

where y is the Compton y parameter, R_v is the virial radius, T_e is the electron temperature, $n_\circ$ is the central electron number density, σ_T is the Thomson cross-section, and $f(\nu)$ is a dimensionless frequency factor (e.g., see Birkinshaw 1999), which we will take to be -2 (i.e., the Rayleigh-Jeans limit). The central decrement is redshift-independent for a given set of cluster properties, allowing a distance-independent probe of cluster properties.

An observable which is more readily interpreted is the integrated SZ flux density from clusters. Assuming that the cluster is approximately isothermal and noting that an integral over solid angle can be written as $d\Omega = dA/d_A^2$, we can write

$$S = S_\circ \int d\Omega \frac{\Delta T}{T_{CMB}} = S_\circ f(\nu) \frac{kT_e}{m_e c^2} \sigma_T \frac{N_e}{d_A^2(z)} \quad , \qquad (3)$$

where N_e is the total number of electrons, d_A is the angular diameter distance and $S_\circ$ gives the conversion from temperature to flux density. At a frequency of 30 GHz, the conversion between flux and $Y \equiv \int y d\Omega$ is approximately $S = 12.7 (Y/arcm^2)$ Jy. The mass distribution does not matter in this case, as long as the integration over solid angle extends to the cluster virial radius and the cluster is roughly isothermal.

The simple relation between the total flux density and the total mass and electron temperature make the SZ a particularly valuable tool for searching for clusters. Cluster detections are largely decoupled from the details of the structure of clusters, allowing an unbiased sample for studies of both cosmology and cluster properties at any redshift.

2.1. *Mass-Temperature Relation*

In connecting with SZ observables, a relation is needed between mass and temperature. Such a relation can be derived from the spherical collapse model (Lahav *et al.* 1991) or can be found from numerical simulations. We have chosen the hybrid approach of Bryan and Norman (1998), where the functional form is taken from the spherical collapse model and the normalization is found from simulations.

Using a notation where $H(z) \equiv 100h\, E(z)$ km s^{-1} Mpc^{-1}, we use

$$T_{gas} = 1.4 \times 10^7 (\Delta(z) E(z)^2)^{\frac{1}{3}} M_{15}^{\frac{2}{3}} \text{ K} \quad , \qquad (4)$$

with M_{15} the virial mass in units of $10^{15} h^{-1} M_\odot$, $\Delta(z)$ is the mean cluster density relative to the critical density at that redshift and the virial radius is defined as the radius that encloses this mean density.

2.2. *Evolution of Cluster Gas*

The SZ observables will be sensitive to the density profile of the ICM, so it is important to model the ICM distribution both as a function of mass and as a function of redshift. The simplest evolution is self-similar evolution, where the central density scales with the background density and sizes will be proportional to the cosmic scale factor. In the absence of physics other than gravity, we would expect something like this sort of evolution, since there is no preferred scale.

It is well-known(e.g., Kaiser 1991; Evrard and Henry 1991; Ponman, Cannon and Navarro 1999) that X-ray observations suggest that gas evolution is not self-similar. If reionization added significant entropy to the gas or if there has been substantial feedback into the ICM from galaxy formation, the excess entropy would shift the ICM to a higher adiabat, leading to a final state of the cluster that is less compact. In such a situation, the outer parts of the cluster might be expected to be largely unchanged, but the details of the cluster profile might depend on the details of the entropy injection (or preferential removal of low entropy gas).

We will assume that the outer parts of clusters are unaffected by feedback or preheating, and approximate the dark matter density profile as a singular isothermal sphere, while the gas density has a well-defined core that is set by the minimum entropy of the gas. For self-similar evolution, this central minimum entropy is set by gravitational processes, while preheated models will have extra entropy injected by other processes, which may or may not be larger than the entropy from gravitational heating.

As a simple model, we adopt the notion of an entropy floor (Ponman, Cannon, and Navarro 1999), where feedback has provided a uniform amount of entropy, and gravitational heating has provided an amount of entropy that increases with increasing mass. This is a slight modification of the constant entropy core model of Evrard and Henry (1991). With an entropy floor rather than a fixed central entropy, high-mass clusters can have a central entropy which is significantly higher than the entropy floor, more in line both with physical intuition and observations.

We define a measure of the entropy as

$$s \equiv \frac{T}{n_e^{2/3}} \quad . \qquad (5)$$

and take the central entropy to be the entropy expected from self-similar evolution plus a constant entropy floor.

The effect of the central entropy floor is to set a maximum central density for a given temperature. For high-mass clusters, the central entropy is set by the gravitational heating; for low-mass clusters, the entropy from gravitational heating is relatively small and the central entropy is determined by the entropy floor, leading to a temperature-dependent central density.

2.2.1. *Self-Similar Evolution*

For self-similar evolution ($s_{floor} = 0$), the core radius should be a fixed fraction of the virial radius. We choose this ratio $\mathcal{R} \equiv R_v/r_c = 10$, in rough agreement with observations of clusters (Mohr, Mathiesen, and Evrard 1999). Under the assumption that the gas density at the virial radius is equal to the global baryon fraction, $f_B \equiv \Omega_B/\Omega_m$, times the mass density at the virial radius, we solve for the central density:

$$n_{\circ;ss} = \frac{f_B}{3\mu_e m_H} \Delta(z) \rho_{crit}(z) (1 + \mathcal{R}^2) \quad . \qquad (6)$$

In general, the global baryon fraction is not equal to the cluster gas mass fraction. Simulations without feedback from galaxy formation typically find values for the cluster gas mass fraction that are only slightly lower than the input global baryon fraction (Evrard 1997). As we outline below, it is possible for the cluster gas mass fraction to deviate strongly from the global baryon fraction if non-gravitational heating is introduced.

The entropy expected from self-similarity for a cluster of a given mass is easily obtained from equation 5 using equations 4 and 6, and can be seen to simply scale with the virial temperature.

The central SZ decrement assuming self-similar evolution and solar abundances of hydrogen and helium ($\mu_e =$

1.14), from equation 2, is

$$\Delta T_\circ = 295\ \mu K\ f_B h\ \frac{1+\mathcal{R}^2}{\mathcal{R}} \arctan\mathcal{R}\ M_{15}\Delta_{178}E(z)^2 \quad . \tag{7}$$

The total flux density, assuming an observing frequency of 30 GHz, can be calculated from equation 3:

$$S = 146\ \mathrm{mJy}\ f_B h\ M_{15}^{5/3}(\Delta_{178}E(z)^2)^{1/3}$$
$$\frac{(1+\mathcal{R}^2)(\mathcal{R}-\tan^{-1}\mathcal{R})}{\mathcal{R}^3}\left(\frac{d_A(z)}{1000h^{-1}\mathrm{Mpc}}\right)^{-2} \quad , \tag{8}$$

where $\Delta_{178} \equiv \Delta/178$. In a universe with $\Omega_m = 1$ the spherical collapse model predicts $\Delta = 178$, with smaller values for low-density universes.

2.2.2. *"Preheated" Models*

For a given temperature, the central density is fixed by the central entropy, and we can use equation 6 to solve for the appropriate value of the core-to-virial ratio $\mathcal{R}$. For the self-similar case the central entropy simply scales with T and $\mathcal{R} = constant$. A non-zero entropy floor breaks the self-similarity and $\mathcal{R}$ becomes a function of temperature. We assume that the entropy from gravitational heating is equal to that expected in the self-similar case and add entropy from non-gravitational heating. We can still use equations 7 and 8, but we must now solve for $\mathcal{R}$ as a function of mass. For low-mass clusters, this leads to significantly different evolution and appearance, as well as a depressed cluster gas mass fraction. As an example, for $\Omega_m = 1$, the self-similar case would predict that the central decrement would scale as $M(1+z)^3$, whereas the entropy floor would predict a scaling as $M^{3/2}(1+z)^{9/4}$. This relation is different in both its mass scaling and its redshift dependence. In this scenario, low-mass high-redshift clusters will be significantly less compact than in a self-similar picture. This would have observable consequences, both in the properties of high-redshift clusters and in their signature in CMB experiments (see §4).

For clusters well below $\sim 10^{14}h^{-1}M_\odot$ the core radius can become significantly larger than the virial radius for high values of the entropy floor. In such cases, the gas distribution is still truncated at the virial radius in our models. This is simply indicating that the entropy of the central gas is sufficiently high that the central density is not significantly higher than the gas density near the virial radius. In this regime, the accretion process could be seriously affected by the entropy floor and it is not clear that our simple model is applicable.

In this work, we assume a relatively high value for the entropy floor of $s_{floor} = 200$ keV cm^2 as an extreme case. Current estimates of the entropy floor (Ponman, Cannon, and Navarro 1999) are roughly $s_{floor} = 100$ keV cm^2.

2.3. *Cosmological Evolution of Cluster Abundances*

We modeled the cosmological evolution of cluster abundances with the Press-Schechter prescription (Press and Schechter 1974; Bond *et al.* 1991), which gives the comoving number density as a function of both mass and redshift. We followed the procedure outlined in Holder et al. (2000), with two minor modifications. The power spectrum was computed using the fitting functions of Eisenstein and Hu (1999), and the redshift evolution of the power spectrum was evaluated numerically from linear theory (e.g., Peebles 1980).

Given the comoving number density, it is straightforward to obtain the number of clusters per steradian above some mass threshold M_{lim} as a simple integral over the comoving number density. To estimate the angular power spectrum of the thermal SZ, we follow Cole and Kaiser (1988), and assume that only Poisson contributions to the angular power spectrum are important.

For this work, we assume that $\Omega_m = 0.3$, $\Omega_\Lambda = 0.7$, $\sigma_8 = 1$ and $h = 0.65$. The expected counts are very sensitive to cosmological parameters, as many authors have found.

3. PROBING HIGH-REDSHIFT CLUSTERS

The effects of preheating on cluster structure can be seen in Figure 1. The largest effects of preheating are seen at low masses and high redshift. These models have been designed to agree with observed properties of X-ray emitting clusters and groups at low redshift, so the true test of these models will be how they fare at high redshift. In particular, important information can be learned about cluster-to-cluster variations in the amount of non-gravitational heating and also in the redshift evolution of the amount of preheating in clusters.

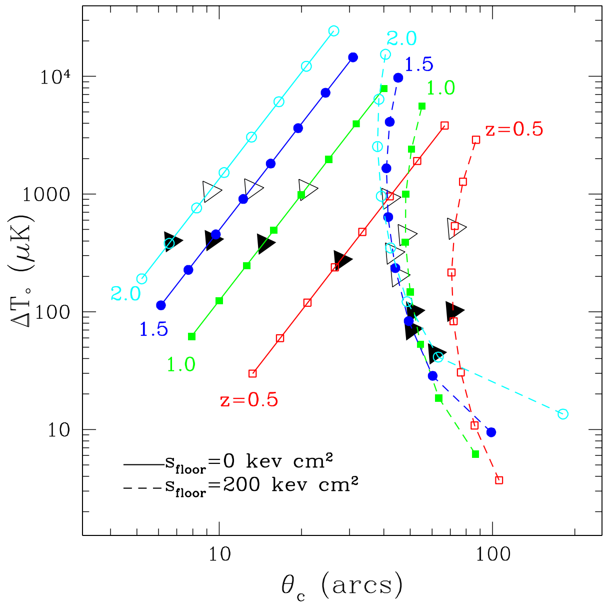

FIG. 1.— Central decrement and core radius for several masses at several redshifts ($z = 0.5, 1, 1.5, 2$) for a preheated model ($s_{floor} = 200$keV cm^2) and self-similar evolution ($s_{floor} = 0$). Mass is marked by open squares along each line and increases along each line from bottom to top in factors of 2, from $0.5 - 64 \times 10^{14}h^{-1}M_\odot$. Lines of constant redshift are marked with similar symbols. Solid (open) triangles mark the limiting mass at which $dN/dz > 1(0.01)$ per square degree per unit redshift for a ΛCDM cosmology.

In Figure 1, we have marked the limiting survey mass at each redshift which is required to obtain a surface density per redshift bin of either 1 or 0.01 clusters per square degree per unit redshift. In order to get a large sample of clusters at high redshift, the survey mass limit must be relatively low.

Typical expected mass limits for SZ surveys are shown in Figure 2. PLANCK is expected to be able to survey most of the sky, at a resolution of $\sim 5'$ down to a level of $\sim 10\mu K$. Deep ground-based surveys should be able to reach a comparable temperature uncertainty on a few tens of square degrees at a resolution of $\sim 1'$.

The SZ is well suited for surveying, with the nice feature that the survey mass limit should be largely decoupled from issues of preheating, as illustrated in Figure 2 by the small difference in the mass limits between the self-similar model and the fairly extreme preheated model.

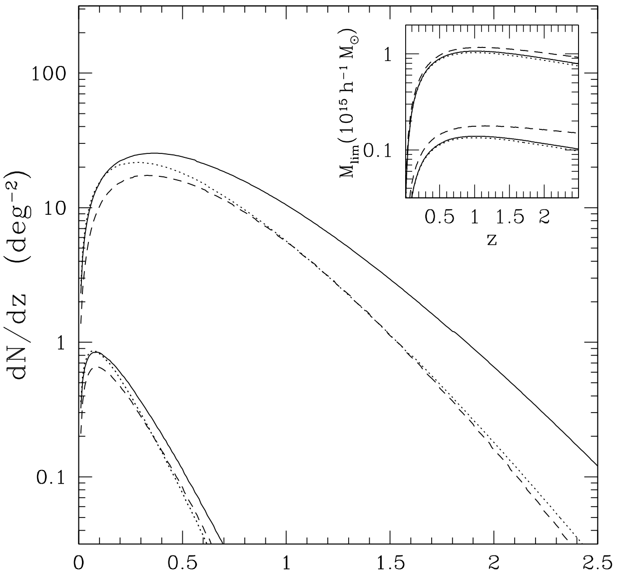

FIG. 2.— Differential number counts of clusters per square degree and mass limits (inset) for SZ surveys for no preheating (solid curve) and significant preheating (dashed curve) for a survey similar to PLANCK (bottom set of lines for dN/dz and top for mass limits) and deep ground-based surveys (top for dN/dz and bottom for mass limits). Flux density units are at 30 GHz ($S \sim 12.7(Y/arcm^2)$). Solid curves assume the ΛCDM cosmology outlined in the text, whereas the dotted curves show self-similar models with $\Omega_m = 0.33$ and $\sigma_8 = 0.9$ and 0.95 for the top and bottom lines in the main panel, respectively.

Redshifts for the clusters will be important to learn about ICM preheating, but it is interesting that a minimum core radius is imposed by preheating which is not very sensitive to redshift. The simple existence of an approximate minimum core radius would be a "smoking gun" for preheating, and the value of this core size is an indicator of the approximate value of the entropy floor. For example, using $s_{floor} = 100$ keV cm^2 will result in a minimum core radius of roughly $30''$. Redshift evolution of the amount of preheating should be observable in the SZ properties of the cluster catalog.

Of particular importance is that preheating should not significantly affect the number of clusters discovered in an SZ survey, only the appearance of the discovered clusters. However, as indicated by the dotted line in Figure 2, the change in expected yields is comparable to the change in yields expected from a shift in Ω_m by 10%. Clearly, non-gravitational heating will be an important consideration when trying to make precise estimates of cosmological parameters from SZ surveys (e.g., Haiman, Mohr, and Holder 2001).

4. SMALL SCALE CMB ANISOTROPY

The structure of high-redshift clusters can have important implications for studies of CMB anisotropies. At small angular scales, the angular power spectrum can become dominated by the thermal SZ effect. The magnitude of the thermal SZ power spectrum is most affected by preheating at exactly the angular scales where it becomes dominant, as shown in Figure 3, as also found in other studies (Holder and Carlstrom 1999; Komatsu and Kitayama 1999; Springel, White, and Hernquist 2000).

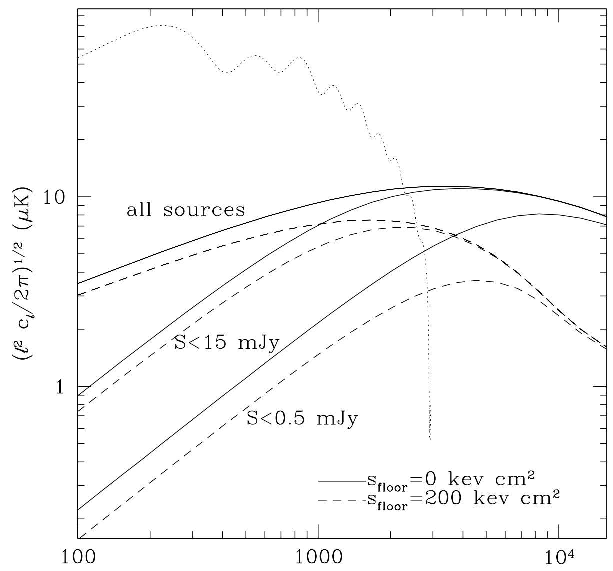

FIG. 3.— Angular power spectrum from SZ clusters. Top solid curve shows the power spectrum due to all SZ clusters in the self-similar model, while the top dashed curve shows the power spectrum from clusters assuming a model with significant preheating. The middle solid curve shows the residual power spectrum for the self-similar model after all SZ clusters brighter than 15 mJy (at 30 GHz) have been removed, with the middle dashed line showing the preheated model. The bottom solid line and dashed curves correspond to the self-similar and preheated models, respectively, after subtraction of all SZ clusters with flux brighter than 0.5 mJy. The expected contribution from primary anisotropies (unlensed) is shown as the light dotted curve, generated by CMBFast (Seljak and Zaldarriaga 1996).

Subtracting out the bright clusters can significantly reduce the power at low multipoles, but does not significantly affect the angular power spectrum at high ℓ, where the thermal SZ effect is expected to exceed the primary anisotropies. The power at high ℓ is mainly due to low-mass clusters at higher z, where non-gravitational heating can be very significant. The higher densities at higher redshift lead to a lower self-similar prediction for the central entropy, making clusters at higher redshift especially sensitive to excess entropy. Deep SZ surveys will allow studies of the clusters which are contributing the majority of the signal at small angular scales. Shallow surveys will detect the clusters which provide the bulk of the power at larger angular scales, where the primary anisotropies are more than an order of magnitude larger than the thermal SZ effect, but will have very little information on the small angular scales at $\ell \gtrsim 2000$.

5. DISCUSSION AND CONCLUSIONS

We have shown that the SZ effect is well-suited for studies of non-gravitational heating. A well-planned survey should not have a selection function which strongly depends on the amount of non-gravitational heating, while SZ images of the resulting catalog will be very sensitive to this energy injection. As a redshift-independent probe, the SZ is particularly well-suited for high-redshift work, where non-gravitational heating can be very important.

We have shown that the expected yield and redshift distribution of clusters for an SZ survey is only weakly sensitive to preheating, but that this sensitivity is significant if one wishes to do "precision cosmology" with SZ surveys. This is true for either deep or shallow surveys. While high-mass clusters are less sensitive to preheating, the survey yield is more sensitive to the mass limit at higher masses. Thus we have a situation where it will be difficult to use high-mass clusters to learn about preheating, but we must understand it to do cosmology. For low-mass clusters, the mass limit is still important for the survey yield, but direct imaging of the resulting catalog of clusters should yield a wealth of information on preheating.

The peak of the SZ angular power spectrum is very sensitive to the details of non-gravitational heating and direct images of high redshift, low mass clusters may be the best way of understanding this signal. Approximately half of the power at $\ell \gtrsim 2000$, where the thermal SZ signal is stronger than the primary anisotropies, should be coming from clusters that could be detected in deep SZ surveys.

Upcoming CMB experiments such as MAP and PLANCK, with their large beam sizes, are not well-suited for finding high redshift and low mass clusters. Ground-based bolometer arrays and interferometers with sub-arcminute resolution will be well equipped for finding and studying these clusters. Deep SZ surveys will happen within the next few years and the information that they yield will be very valuable for constraining non-gravitational heating through galaxy formation or reionization. This information should be remarkably unbiased, and improvements in SZ imaging over the next several years should continue to improve our understanding of these processes.

This is work supported by NASA LTSA grant number NAG5-7986 and the DOE at Chicago. We acknowledge many useful discussions with Joe Mohr and thank U. Seljak and M. Zaldarriaga for making CMBFast publicly available.

REFERENCES

Balogh, M., Babul, A., and Patton, D. 1999, MNRAS, 307, 463.
Barbosa, D., Bartlett, J., Blanchard, A., and Oukbir, J. 1996, A&A, 314, 13.
Bartlett, J.G. 2000, A&A, submitted.
Birkinshaw, M. 1999, Physics Reports, 310, 97.
Bond, J., Kaiser, N., Cole, S., and Efstathiou, G. 1991, ApJ, 379, 440.
Bower, R., Benson, A., Baugh, C., Cole, S., Frenk, C., and Lacey, C. 2000, MNRAS, submitted, astro–ph/0006109.
Bryan, G. and Norman, M. 1998, ApJ, 495, 80.
Bryan, G. 2000, ApJ, 544, L1.
Carlstrom, J. E., Joy, M., Grego, L., Holder, G., Holzapfel, W. L., LaRoque, S., Mohr, J. J., and Reese, E. D. 2000. In Durret, F. and Gerbal, G., editors, *Constructing the Universe with Clusters of Galaxies*, IAP, astro-ph/0103480 .
Cavaliere, A., Menci, N., and Tozzi, P. 1999, MNRAS, 308, 599.
Cole, S. and Kaiser, N. 1988, MNRAS, 233, 637.
Eisenstein, D. J. and Hu, W. 1999, ApJ, 511, 5.
Evrard, A. and Henry, J. 1991, ApJ, 383, 95.
Evrard, A. 1997, MNRAS, 292, 289.
Grego, L., Carlstrom, J. E., Reese, E. D., Holder, G. P., Holzapfel, W. L., Joy, M. K., Mohr, J. J., and Patel, S. 2001, ApJ, page in press.
Haiman, Z., Mohr, J. J., and Holder, G. P. 2001, ApJ, in press: astro-ph/0002336.
Holder, G. and Carlstrom, J. 1999, in Microwave Foregrounds, ed. A. de Oliveira-Costa and M. Tegmark (San Francisco. ASP), 199, astro-ph/9904220.
Holder, G. P., Mohr, J. J., Carlstrom, J. E., E., E. A., and Leitch, E. M. 2000, ApJ, 544, 629.
Irwin, J. A. and Bregman, J. N. 2000, ApJ, 538, 543.
Kaiser, N. 1991, ApJ, 383, 104.
Kneissl, R., Jones, M. E., Saunders, R., Eke, V. R., Lasenby, A. N., Grainge, K., and Cotter, G. 2001, submitted: MNRAS. astro-ph/0103042.
Komatsu, E. and Kitayama, T. 1999, ApJ, 526, L1.
Lahav, O., Rees, M. J., Lilje, P. B., and Primack, J. R. 1991, MNRAS, 251, 128.
Mohr, J., Mathiesen, B., and Evrard, A. 1999, ApJ, 517, 627.
Peebles, P.J.E. 1980. *The Large Scale Structure of the Universe*. Princeton University Press, Princeton.
Ponman, T. J., Cannon, D. B., and Navarro, J. F. 1999, Nature, 397, 135.
Press, W. and Schechter, P. 1974, ApJ, 187, 425.
Reese, E. D. *et al.* 2000, ApJ, 533, 38.
Seljak, U. and Zaldarriaga, M. 1996, ApJ, 469, 437.
Springel, V., White, M., and Hernquist, L. 2000, ApJ, submitted, astro–ph/0008133.